Intermodulation in Heterojunction Bipolar Transistors

Stephen A. Maas, *Senior Member, IEEE,* Bradford L. Nelson, *Member, IEEE,* and Donald L. Tait, *Member, IEEE*

***Abstract*—This paper examines the modeling of small-signal intermodulation distortion (IM) in heterojunction bipolar transistors (HBT's). We show that IM current generated in the exponential junction is partially cancelled by IM current generated in the junction capacitance, and that this phenomenon is largely responsible for the unusually good IM performance of these devices. Thus, a nonlinear model of the HBT must characterize both nonlinearities accurately. Finally we propose a nonlinear HBT model suitable for IM calculations, show how to measure its parameters, and verify its accuracy experimentally.**

I. Introduction

ONE OF the most delightful properties of the heterojunction bipolar transistor (HBT) is its unusually high linearity at relatively low levels of dc bias power. For example, Nelson *et al.* have reported a third-order intermodulation intercept point (IP_3) of 33 dBm in a small-signal amplifier using two HBTs and 150 mW dc power [1]; other researchers have reported similar results [2]. This high linearity is surprising in view of the fact that the dependence of the HBT's emitter current, I_e, on base-to-emitter voltage, V_{be}, is an exponential function, one of the strongest nonlinearities found in nature. Furthermore, the junction capacitance, primarily a diffusion capacitance, is also very strongly nonlinear.

The reason for this unusually high linearity has never been explained adequately. It has been addressed to some degree in papers on the modeling of intermodulation distortion (IM) in homojunction bipolar transistors (BJTs) [3]–[7]. One of the most common explanations is that the output resistance of these devices is very high, and thus does not generate IM current. Although it is true that the nonlinearity of the output resistance is not a dominant contributor to IM in HBTs, it is not clear why the more strongly nonlinear $I_e(V_{be})$ does not still provide very high levels of distortion.

A Volterra-series analysis of a simplified HBT equivalent circuit has been used to resolve this quandary. It leads to a surprising and thoroughly counterintuitive conclusion: as long as the dominant frequency components are below the transistor's current-gain cutoff frequency f_t (which in our devices is ~ 50 GHz), the largest output-current distortion components generated by the resistive junction and those generated by the junction capacitance have a 180-degree phase difference, and, in theory, cancel almost exactly. Thus, paradoxically, it is the strong nonlinearity of both elements that causes the IM levels to be low; if only one of these elements were nonlinear, the device's intermodulation would be much greater.

Relatively few nonlinear models of HBTs have been reported, and none of these have been intended specifically for IM analysis [2], [8], [9]; indeed, the requirements of a device model for accurate IM calculations are generally more severe than for single-tone, large-signal amplifier analysis [10]. Here we propose such a model, and demonstrate its validity experimentally.

Manuscript received May 3, 1991; revised July 10, 1991. This work was supported by TRW, Inc. under independent research and development funds.

S. A. Maas is with the Department of Electrical Engineering, University of California, Los Angeles, Los Angeles, CA 90024-1594.

B. L. Nelson and D. L. Tait are with TRW, Inc., One Space Park, Redondo Beach, CA 90278.

IEEE Log Number 9105708.

II. Intermodulation in the HBT

We now examine analytically the distortion processes in a bipolar device. We do this by performing a Volterra-series analysis of a simplified HBT equivalent circuit, using the method of nonlinear currents [11]–[13]. Although the equivalent circuit we use is somewhat idealized and some significant nonlinearities are not included, it nevertheless illustrates a remarkable property of the device: the cancellation of distortion components generated in the resistive and reactive parts of the junction.

Consider the simplified equivalent circuit of an HBT shown in Fig. 1. The transistor has real source and load impedances (this assumption is not a very restrictive; we shall examine it later). The resistance R_b represents the sum of the base resistance and the source resistance; the load resistance is R_L. The nonlinearities are modeled by a resistive diode (the base-to-emitter junction) and a nonlinear capacitance. Under small-signal conditions, the junction I/V characteristic can be expanded in a Taylor series in the vicinity of its bias point, yielding

$$i_g = g_1 v + g_2 v^2 + g_3 v^3 \tag{1}$$

where I_0 is the saturation current and δ is the quantity q/ηKT. In the HBT η is very close to 1.0; also $g_1 = 1/R_{je}$, the inverse of the linearized junction resistance. Similarly, in the vicinity of its bias point the junction capacitance has the small-signal charge/voltage characteristic

$$I_e = I_0(\exp(\delta V_{be}) - 1) \tag{2}$$

where I_0 is the saturation current and δ is the quantity q/ηKT. In the HBT η is very close to 1.0; also $g_1 = 1/R_{je}$, the inverse of the linearized junction resistance. Similarly, in the vicinity of its bias point the

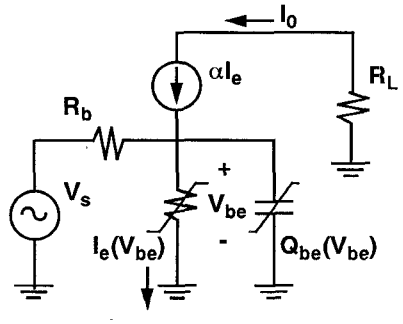

Fig. 1. Simplified, linearized equivalent circuit of the HBT. $I_e(V_{be})$ represents the resistive base-to-emitter junction, and $Q_{be}(V_{be})$ represents the charge in the capacitive part of the junction.

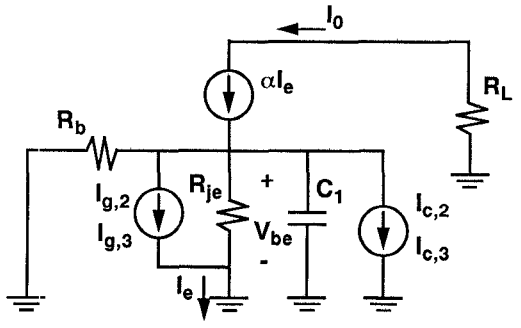

Fig. 2. Equivalent circuit of the HBT used for intermodulation analysis. The current sources $I_{c,2}$ and $I_{c,3}$ are the second- and third-order nonlinear current sources, respectively, representing the junction capacitance; $I_{g,2}$ and $I_{g,3}$ are those representing the resistive junction.

junction capacitance has the small-signal charge/voltage characteristic

$$q_{be} = c_1 v + c_2 v^2 + c_3 v^3 \tag{3}$$

where c_n, like g_n, are Taylor-series coefficients. The small-signal current in the capacitance is dq_{be}/dt. If we temporarily make the assumption that the base-to-emitter capacitance is dominated by diffusion capacitance, the large-signal charge $Q_{be}(V_{be})$ is

$$Q_{be}(V_{be}) = \tau I_e \tag{4}$$

where τ is a constant with units of time. In reality the base-to-emitter charge has a substantial depletion component, and often is not dominated by diffusion charge storage. We shall consider this matter later.

The coefficient $c_1 = (d/dV_{be})Q_{be}(V_{be})$ in (3), together with the expression for charge in (4), is the linearized junction capacitance.

This expression, (4), represents an oversimplification of the nonlinear capacitance in a bipolar device: it does not include the depletion capacitance, and in any case is valid only when τ is much less than a period of the excitation voltage. Also, the capacitive nonlinearity is much weaker than (4) implies. (Nevertheless, this expression is used commonly in linear and nonlinear circuit simulators, notably in SPICE II [3], to model intermodulation distortion in bipolar devices.)

If the common-base current gain $\alpha \cong 1$, the first-order base-to-emitter voltage $V_{be,q}$ at the excitation frequency ω_q can be expressed by

$$V_{be,q} = \frac{V_s}{1 + R_b c_1 j\omega_q}. \tag{5}$$

We find the second-order voltage by means of Volterra-series analysis and the method of nonlinear currents [13]–[15]. The equivalent circuit for second-order products is shown in Fig. 2. The second-order currents in the excitation sources associated with the resistive nonlinearity, $I_{g,2}$, and the capacitive nonlinearity, $I_{c,2}$, (the "nonlinear currents") are

$$I_{g,2} = \tfrac{1}{4} g_2 \sum_{q_1=-Q}^{Q} \sum_{q_2=-Q}^{Q} V_{be,q_1} V_{be,q_2} \exp\left(j(\omega_{q_1} + \omega_{q_2})t\right) \tag{6}$$

$$I_{c,2} = \tfrac{1}{4} c_2 \sum_{q_1=-Q}^{Q} \sum_{q_2=-Q}^{Q} V_{be,q_1} V_{be,q_2} (j(\omega_{q_1} + \omega_{q_2})) \cdot \exp\left(j(\omega_{q_1} + \omega_{q_2})t\right) \tag{7}$$

where V_{be,q_1} is the first-order voltage phasor of V_{be} at the excitation frequency ω_{q_1}, and there are Q excitation frequencies. When only a single excitation frequency ω_1 exists, the second-harmonic component of the current in the resistive part of the junction is

$$I_{g,2}(2\omega_1) = \frac{g_2 V_{be,1}^2}{2} \tag{8}$$

and the second-harmonic component in the base-to-emitter capacitance is

$$I_{c,2}(2\omega_1) = j\omega_1 c_2 V_{be,1}^2. \tag{9}$$

(Since we will be concerned with no other second-order currents, from now on we will use $I_{g,2}$ and $I_{c,2}$ to represent the second-harmonic IM components.)

Performing a linear analysis of this circuit, we find the junction voltage at the second harmonic, $2\omega_1$. It is

$$V_{be}(2\omega_1) = \frac{-(I_{c,2} + (1-\alpha)I_{g,2})}{2c_1 j\omega_1} \tag{10}$$

where we have again used the approximation $\alpha \cong 1$ and assumed that $2R_b c_1 \omega_1 >> 1$. The output current $I_{o,2}$ at this second-harmonic frequency is

$$I_{o,2} = \alpha I_{e,2} = \alpha\left(I_{g,2} + \frac{V_{be}(2\omega_1)}{R_{je}}\right). \tag{11}$$

Substituting (8)–(10) into (11) gives

$$I_{o,2} = \frac{\alpha V_{be,1}^2}{2R_{je}c_1}(R_{je}c_1 g_2 - c_2) - \frac{\alpha V_{be,1}^2 (1-\alpha) g_2}{4R_{je}c_1 j\omega_1}. \tag{12}$$

The first term in (12) is interesting for a number of reasons. First, although it depends in part on the junction capacitance, it is frequency-independent; $j\omega_1$ terms in the numerator and denominator have cancelled. Thus, the second term, which includes $j\omega_1$ in the denominator, is comparatively small (at microwave frequencies it is virtually always negligible). Second, the second-order cur-

rent components arising in the resistive junction, described by $R_{je}c_1g_2$, have either a zero or 180-degree phase relationship with those arising in the junction capacitance, described by c_2. Therefore, if c_1g_2 and c_2 are both positive (which, in fact, they are), the second-order components of distortion current cancel.

Differentiating (2) and (4), we find the c_n and g_n coefficients in (1) and (3) to be

$$1/R_{je} = g_1 = \delta I_e, \quad g_2 = \delta^2 I_e/2, \quad g_3 = \delta^3 I_e/6,$$
$$c_1 = \tau\delta I_e, \quad c_2 = \tau\delta^2 I_e/2, \quad c_3 = \tau\delta^3 I_e/6 \tag{13}$$

Substituting these into (12), we find that the term $(\alpha V_{be,1}^2/2R_{je}c_1)(R_{je}c_1g_2 - c_2)$ cancels *exactly*, leaving only the negligible second term.

Unfortunately, for a number of reasons this cancellation is incomplete in real devices. First, we have already mentioned the imperfection of (4) for describing the base-to-emitter junction diffusion capacitance. This capacitance includes a substantial depletion component, which we did not include; replacing part of this ideal diffusion capacitance by the more weakly nonlinear depletion capacitance reduces the strength of the capacitive nonlinearity. Second, although (2) describes the emitter current accurately in GaAs–AlGaAs HBT's, the collector current is not well described by the relation $I_c = \alpha I_e$; this relationship is weakly but not negligibly nonlinear, and includes a time delay t_d. Thus we must use an expression of the form

$$I_c = \alpha_1 I_e(t - t_d) + \alpha_2 I_e^2(t - t_d) + \alpha_3 I_e^3(t - t_d) + \cdots \tag{14}$$

to describe the relationship between small-signal collector and emitter currents. Finally, this theoretically perfect cancellation occurs only when all significant frequency components are within the mid-frequency range. It would not occur, for example, in the case of a two-tone component at $\omega_1 - \omega_2$, where ω_1 and ω_2 are closely spaced excitation frequencies, or in higher-order multitone products where such low-order components are significant contributors. Nevertheless, substantial cancellation clearly occurs in practical devices: the difference between the second-order (i.e., second-harmonic) intercept point at low frequencies (where the base-to-emitter capacitance is negligible) and at mid frequencies (where $2\omega_1 > 1/R_bc_1$) is on the order of several dB.

(It is interesting—and perhaps tantalizing—to note that if this cancellation were perfect, the mid-frequency second-order intercept points would be on the order of 50 dB or more. Thus, it may be possible to improve the linearity of these devices by closely matching their capacitive and reactive nonlinearities.)

Cancellation of the distortion currents occurs in third-order products as well. Since third-harmonic cancellation process is nearly identical to second-harmonic, we illustrate this phenomenon briefly by considering the more interesting third-order IM product at $2\omega_2 - \omega_1$. The equivalent circuit of Fig. 2 is valid for third-order IM as well as second, as long as the nonlinear currents in the resistive and reactive parts of the junction, $I_{g,3}$ and $I_{c,3}$ respectively, are expressed by

$$I_{g,3} = \frac{3g_3}{4} V_{be,1}^* V_{be,2}^2 + g_2(V_{be,1}^* V_{be}(2\omega_2) + V_{be,2}V_{be}(\omega_2 - \omega_1)) \tag{15}$$

$$I_{c,3} = j(2\omega_2 - \omega_1)\left[\frac{3c_3}{4} V_{be,1}^* V_{be,2}^2 + c_2(V_{be,1}^* V_{be}(2\omega_2) + V_{be,2}V_{be}(\omega_2 - \omega_1))\right] \tag{16}$$

and the third-order junction voltage, $V_{be}(2\omega_2 - \omega_1)$, is

$$V_{be}(2\omega_2 - \omega_1) = \frac{-(I_{c,3} + (1 - \alpha)I_{g,3})}{c_1(2\omega_2 - \omega_1)}. \tag{17}$$

The output current, $I_{o,3}$, is

$$I_{o,3} = \alpha I_{e,3} = \alpha\left(I_{g,3} + \frac{V_{be}(2\omega_2 - \omega_1)}{R_{je}}\right). \tag{18}$$

Substituting (15)–(17) into (18) gives

$$I_{o,3} = \frac{\alpha}{R_e c_1 j(2\omega_2 - \omega_1)}\left[\left((R_{je}c_1(2\omega_2 - \omega_1) - (1 - \alpha)) \cdot \left(\frac{3g_3}{4} V_{be,1}^* V_{be,2}^2 + g_2(V_{be,1}^* V_{be}(2\omega_2) + V_{be,2}V_{be}(\omega_2 - \omega_1))\right) - \frac{3j(2\omega_2 - \omega_1)}{4} \cdot c_3 V_{be,1}^* V_{be,2}^2 - j(2\omega_2 - \omega_1)c_2(V_{be,1}^* V_{be}(2\omega_2) + V_{be,2}V_{be}(\omega_2 - \omega_1))\right]. \tag{19}$$

In the above expression we have stretched our assumptions a trifle by implicitly assuming that the $\omega_2 - \omega_1$ component is within the mid-frequency range, although in practice it rarely is. Because the terms in (19) containing this term are not dominant, the inaccuracy thus introduced is not great. Our purpose is to illustrate the existence of cancellation effects in third-order intermodulation, not to calculate IM levels exactly; thus, we will allow ourselves this liberty.

Under the same assumptions as for the second-order component, $g_3 = \delta^3 I_e/6$ and $c_3 = \tau\delta^3 I_e/6$. Substituting these into (19), we find that many of the terms cancel (in fact, all the terms containing τ cancel) and we obtain for $I_{o,3}$:

$$I_{o,3} = \frac{-\alpha(\alpha - 1)}{2R_e c_1 j(2\omega_2 - \omega_1)} \delta^2 I_e\left(\frac{3}{4}\delta V_{3a} + V_{3b}\right) \tag{20}$$

where

$$V_{3a} = V_{be,1}^* V_{be,2}^2$$

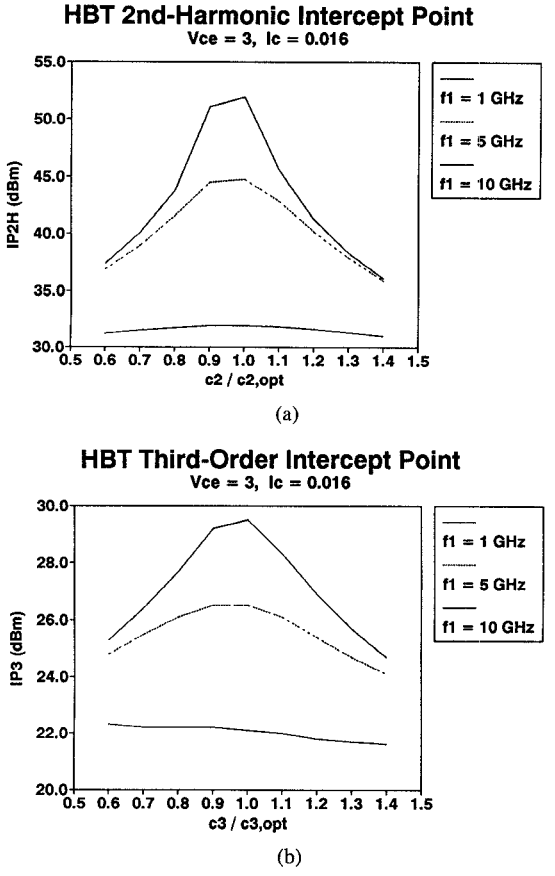

Fig. 3. (a) Second-harmonic and (b) third-order intercept points as functions of $c_2/c_{2,\mathrm{opt}}$ and $c_3/c_{3,\mathrm{opt}}$ when $Z_s = Z_l = 50\ \Omega$.

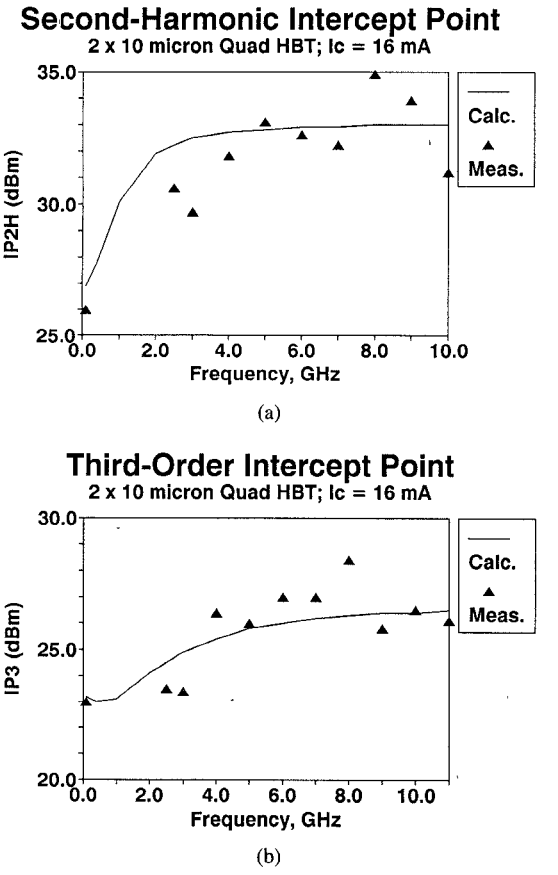

Fig. 4. Measured and calculated IP_2 (a) and IP_3 (b) of a TRW 2 × 10 μm quad-emitter HBT. The second-order product is the second harmonic of the excitation frequency, and the third-order product is the one at $2\omega_2 - \omega_1$. The bias conditions are $I_c = 16$ mA, $V_{ce} = 3$ V, and $Z_s = Z_l = 50\ \Omega$.

and

$$V_{3b} = V^*_{be,1} V_{be}(2\omega_2) + V_{be,2} V_{be}(\omega_2 - \omega_1).$$

Fig. 3 shows the calculated second- and third-order intercept points of a 2 × 10 μm quad-emitter HBT, as a function of the capacitance coefficients $c_2/c_{2,\mathrm{opt}}$ and $c_3/c_{3,\mathrm{opt}}$, where $c_{n,\mathrm{opt}}$ is the optimum value of c_n, given by (3) and (13). The HBT is modeled by the complete equivalent circuit (described in Section III, below). It is clear from these plots that, even with the HBT's parasitics, the capacitance given by (4) is the value that provides optimum IP_2. It also shows that $c_{2,\mathrm{opt}}$, as predicted by (12), is largely independent of frequency as long as the device is operated well above the cutoff frequency for such phenomena, i.e., $\omega_1 >> 1/R_b c_1$.

Fig. 4 shows the measured second- and third-order intercept points of the 2 × 10 μm quad-emitter HBT biased at 3 V, 16 mA collector current, and having 50-Ω source and load impedances. These are compared to the intercept points calculated for the full equivalent circuit described in the next section. The IM calculations were performed by the Volterra-series program C/NL [16]. At low frequencies the intercept points are relatively low, because the IM currents in the resistive junction are not cancelled by those of the capacitive junction (the cutoff frequency for cancellation effects, $1/2\pi R_b c_1$, is approximately 1 GHz). Above this frequency the second- and third-order intercept points rise; they eventually level off at a value that remains remarkably constant with further increases in frequency.

The worst-case difference between the calculated and measured intercept points in Fig. 4 is approximately 2 dB, although most points are within 1 dB. We believe that this error is caused primarily by difficulty in controlling of the source and load impedances during the measurement: the calculations were made under the assumption that the source and load impedances were 50 Ω; however, the measurements were made on-wafer with probes having VSWR's as high as 2.0 at some frequencies.

The previous analysis was based on an assumption that the source impedance was large and real, typically 50 Ω. In practical situations, where the source impedance is complex, one might be tempted to question the validity of the above analysis. The cancellation effects described above occur when the dominant components of the harmonics or IM distortion occur at frequencies where the reactance of the junction capacitance is much less than $\mathrm{Re}\ \{Z_s\} + R_{b1} + R_{b2}$ (where Z_s is the source impedance and $R_{b1} + R_{b2}$ are as shown in Fig. 5), and most of the current of the nonlinear current sources in Fig. 2 circulates in R_{je} and C_{be}. This is usually the case at microwave frequencies when the input is conjugate matched. The load impedance has a strong effect on the device's intercept

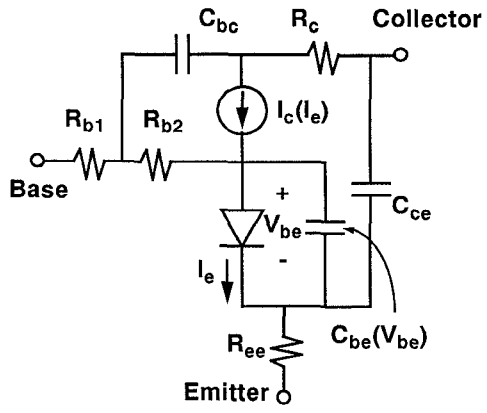

Fig. 5. Complete nonlinear equivalent circuit of the HBT.

points; however, it does not affect the existence of the cancellation phenomena we have described.

III. Modeling the HBT

To model the HBT we use the equivalent circuit of Fig. 5. This circuit includes three nonlinearities: the resistive junction, modeled as an ideal junction diode, the capacitive junction, and the nonlinear current source $I_c(I_e)$. We also include a number of parasitics that were not part of the simplified circuit of Fig. 1; the most important of these is the emitter resistance R_{ee}.

The parameters of the model are found from a combination of dc and S-parameter measurements. We have measured the parameters of the junction I/V characteristic in two ways. The first is to plot log (I_e) as a function of V_{be} at low current levels (so-called Gummel plots). If the junction temperature remains constant over an adequate range of bias voltages, the parameters of (2) can be found from such a plot in a straightforward manner [17]. However, our HBT's have a junction-to-mounting surface thermal resistance of 600–1000 centigrade degrees per watt (depending on device size), and are therefore subject to considerable junction heating. Because the parameter I_o is very sensitive to temperature, it is not possible to find R_{ee} from such a plot; instead, we use the device's low-frequency Z parameters to find R_{ee}. We first convert measured low-frequency S parameters to Z parameters, then find R_{ee} from a plot of Z_{12} as a function of $1/I_e$. This plot is the straight line $Z_{12} = R_{je} + R_{ee}$, and the extrapolated y-intercept is R_{ee}. This method eliminates the effects of junction heating on the parameter I_o in (2); the effects of temperature on δ are not eliminated, but they are not severe enough to affect the measurement of R_{ee} significantly.

(One might object that the HBT's equivalent circuit [Fig. 5] does not have a Z matrix, and thus Z_{12} is undefined. However, the real device has a finite albeit large collector-to-base resistance; this resistance allows Z_{12} to be defined. Numerical tests have shown that a resistance of even several megohms results in a well conditioned Z matrix. We do not include it in the model, however, because its effects on other aspects of the device's performance are thoroughly inconsequential.)

The collector current I_c is a nonlinear function of emitter current I_e, and there is a time delay t_d between the two currents. Because of numerical difficulties in differentiating $I_c(I_e)$, the nonlinearity in α is best found by differentiating $\beta(I_e)$. We find $\beta(I_e)$ by converting low-frequency S parameters, measured at several values of I_e, to H parameters; then $\beta \equiv H_{21}$. The Taylor-series expression for I_c has a delay t_d and the coefficients α_n:

$$I_c = \alpha_1 I_e(t - t_d) + \alpha_2 I_e^2(t - t_d) + \alpha_3 I_e^3(t - t_d) \quad (21)$$

where

$$\alpha_n = \frac{1}{n!}\frac{d^n}{dI_e^n} I_c. \quad (22)$$

The α coefficients are given in terms of β by

$$\alpha_1 = \frac{\beta}{\beta + 1} \quad (23)$$

$$\alpha_2 = \frac{1}{2(\beta + 1)^2}\frac{d\beta}{dI_e} \quad (24)$$

$$\alpha_3 = \frac{1}{6(\beta + 1)^2}\left(\frac{-2}{\beta + 1}\frac{d\beta}{dI_e} + \frac{d^2\beta}{dI_e^2}\right). \quad (25)$$

The time delay t_d can be found by fitting S parameters measured over a range of microwave frequencies to those calculated from the equivalent circuit of Fig. 5. The circuit's S parameters and distortion are surprisingly sensitive to t_d; a change of even a few picoseconds significantly affects both the S parameters and the IM intercept points.

The nonlinear base-to-emitter capacitance $C_{be}(V_{be})$ is the parameter most difficult to model. We use (3) to model the capacitance and determine the c_n coefficients at each bias point of interest by measurement. The first coefficient, c_1, is the linear base-to-emitter capacitance; it is found by fitting the model to measured S parameters. Once the α_n and $I_e(V_{be})$ are established, c_2 is the only parameter affecting second-order intermodulation; therefore it can be adjusted so that calculated and measured IM levels are identical at some convenient point in the mid-frequency region (the measurements are made with 50-Ω source and load impedances). Similarly, when c_2 is known, the only remaining parameter affecting third-order IM is c_3; this parameter is adjusted to give the correct third-order IM levels.

IV. Results

Table I shows the model parameters for a TRW 2 × 10 μm quad-emitter HBT. This device has a vertical structure similar to that described by described by Nelson *et al.* [1] and Kim *et al.* [2]; however its emitter area is somewhat greater. The results shown in Figs. 3–6 were obtained through the use of the data in Table I.

This model has been used to predict the second- and third-order intercept points of a monolithic HBT

TABLE I
EQUIVALENT-CIRCUIT PARAMETERS OF A TRW 2 × 10 μm QUAD (i.e., FOUR-EMITTER) HBT

Parameter	Value
R_{ee}	1.7
R_{je}	1.75
R_{b1}	3.7
R_{b2}	3.7
R_c	3.0
C_{bc}	$58.7 \cdot 10^{-15}$
C_{ce}	$15.7 \cdot 10^{-15}$
η	1.065
I_o	$1.0 \cdot 10^{-23}$
c_1	$1.85 \cdot 10^{-12}$
c_2	$1.2 \cdot 10^{-11}$
c_3	$4.0 \cdot 10^{-11}$
α_1	0.9764
α_2	0.22605
α_3	−6.259
t_d	$3.66 \cdot 10^{-12}$

$V_{ce} = 3.0$, $I_c = 16$ mA, $T_j = 305$°K (estimated junction temperature).

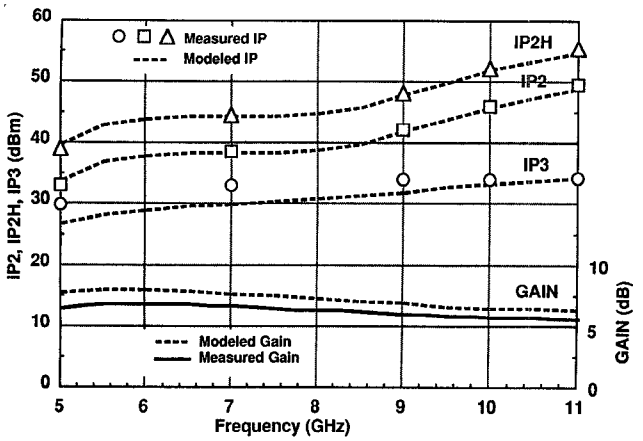

Fig. 6. Comparison of measured and modeled gain, IP_2, and IP_3 of a single-stage, quadrature-coupled HBT amplifier.

amplifier. The amplifier is a single-stage, quadrature-coupled unit; Fig. 6 compares its measured and calculated second- and third-order intercept points. The intermodulation calculations were made by the harmonic-balance program Libra [18]; the HBT model was installed in it as a "user-defined" model, and the circuit was analyzed as a whole; i.e., both devices and all passive elements were included. The accuracies of the gain and two second-order IM products are well within 1 dB, and the calculated and measured third-order intercept points are within two dB of each other.

V. CONCLUSION

This paper has shown that intermodulation distortion can be modeled in an HBT by considering three nonlinearities: the resistive and reactive parts of the base-to-emitter junction and the current-gain nonlinearity. The IM distortion of these devices is low because of cancellation of IM components arising in the nonlinear base-to-emitter junction resistance and capacitance. Finally, we have shown that the device can be modeled accurately by a straightforward equivalent circuit, and the parameters of that circuit can be extracted from RF and dc measurements. These results inevitably suggest that intermodulation distortion can be reduced further by increasing—rather than decreasing—the strength of the capacitive nonlinearity.

ACKNOWLEDGMENT

The authors would like to thank Wes Yamasaki of TRW for assistance with measurements. We would also like to thank Aaron Oki and Dwight Streit of TRW for providing devices, and for helpful discussions the following: R. J. Trew of North Carolina State University, D. S. Pan of UCLA, and Carol Brunnenmeyer, P. Chris Grossman, Mike Kim, and Dave Neilson of TRW.

REFERENCES

[1] B. L. Nelson *et al.*, "High-linearity, low dc power GaAs HBT broadband amplifiers to 11 GHz," in *1989 IEEE Gallium Arsenide Integrated Circuits Symp. Tech. Dig.*, Oct. 1989.
[2] M. E. Kim *et al.*, "12-40 GHz low harmonic distortion and phase noise performance of GaAs heterojunction bipolar transistors," *1988 IEEE GaAs IC Symp. Dig.*, p. 117.
[3] S. H. Chisolm and L. W. Nagel, "Efficient computer simulation of distortion in electronic circuits," *IEEE Trans. Circuit Theory*, vol. CT-20, no. 6, p. 742, Nov. 1973.
[4] S. Narayanan, "Transistor distortion analysis using Volterra series representation," *Bell Syst. Tech. J.*, vol. 46, no. 3, p. 991, May/June 1967.
[5] H. C. Poon, "Modeling of bipolar transistor using integral charge-control model with application to third-order distortion studies," *IEEE Trans. Electron Devices*, vol. ED-19, no. 6, p. 719, June 1972.
[6] J. W. Graham, L. Ehrman, "Nonlinear systems modeling and analysis with applications to communications receivers," Rome Air Development Center, Tech. Rep. RADC AD-766278, 1973.
[7] D. D. Weiner and J. E. Spina, *Sinusoidal Analysis and Modeling of Weakly Nonlinear Circuits*. New York: Van Nostrand Reinhold, 1980.
[8] C. T. Matsuno, A. K. Sharma, and A. K. Oki, "A large-signal HSPICE model for the heterojunction bipolar transistor," *IEEE Trans. Microwave Theory Tech.*, vol. 37, no. 9, p. 1472, Sept. 1989.
[9] M. E. Hafizi, C. R. Crowell, and M. E. Grupen, "The dc characteristics of GaAs/AlGaAs heterojunction bipolar transistors with application to device modeling," *IEEE Trans. Electron Devices*, vol. 37, no. 10, p. 2121, Oct. 1990.
[10] S. A. Maas and D. Neilson, "Modeling MESFETs for intermodulation analysis of mixers and amplifiers," in *1990 IEEE MTT-S Int. Microwave Symp. Dig.*, p. 1291.
[11] M. Schetzen, "Multilinear theory of nonlinear networks," *J. Franklin Institute*, vol. 320, no. 5, p. 221, Nov. 1985.
[12] J. J. Bussgang, L. Ehrman, and J. W. Graham, "Analysis of nonlinear systems with multiple inputs," *Proc. IEEE*, vol. 62, no. 8, p. 1088, Aug. 1974.
[13] S. A. Maas, *Nonlinear Microwave Circuits*, Norwood, MA: Artech House, 1988.
[14] ——, "A general-purpose computer program for the Volterra-series analysis of nonlinear microwave circuits," in *1988 IEEE MTT-S Int. Microwave Symp. Dig.*, p 311.
[15] A. M. Khadr and R. H. Johnston, "Distortion in high-frequency FET amplifiers," *IEEE J. Solid-State Circuits*, vol. SC-9, no. 4, p. 180, Aug. 1974.
[16] S. A. Maas, *C/NL: Linear and Nonlinear Microwave Circuit Analysis and Optimization Software*, Norwood, MA: Artech House, 1990.
[17] ——, *Microwave Mixers*, Norwood, MA: Artech House, 1986.
[18] EEsof, Inc., Westlake Village, CA.

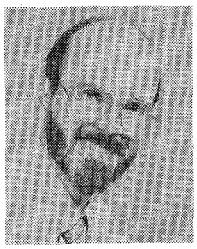

Stephen A. Maas (S'80–M'83–SM'89) was born in Quincy, MA in 1949. He received B.S.E.E. and M.S.E.E. degrees in electrical engineering from the University of Pennsylvania in 1971 and 1972, respectively, and the Ph.D. degree in electrical engineering from UCLA in 1984.

He has been involved in research and development of low-noise and wide-dynamic-range receiving systems and components for radio astronomy and space communication at several institutions. At the National Radio Astronomy Observatory he was responsible for the design of the low-noise receivers for the very large array radiotelescope. At Hughes Aircraft Co. and TRW he developed low-noise microwave and millimeter-wave systems and components, primarily FET amplifiers and diode and FET mixers, for space communication. Most recently he was a Research Scientist at The Aerospace Corp., where his primary interests involved the optimization of nonlinear microwave circuits and the development of circuit-design software based on harmonic-balance, Volterra-series, and time-domain methods. He now is a member of the Electrical Engineering Faculty at UCLA and consults for companies in the Los Angeles area.

Dr. Maas is the author of *Microwave Mixers* (Artech House, 1986) and *Nonlinear Microwave Circuits* (Artech House, 1988), and currently is the Editor of the IEEE TRANSACTIONS ON MICROWAVE THEORY AND TECHNIQUES.

Brad L. Nelson (M'90) was born in San Diego, CA in Feb. of 1962. In 1985 he received his B.S. degree in engineering physics from the University of the Pacific, Stockton, CA. He is currently working on the M.S. degree in electrical engineering at the University of Southern California.

From 1983 to 1984 he worked at Naval Ocean Systems Center, San Diego, CA on ocean sensor arrays. In 1984 he joined TRW, Redondo Beach, CA. At TRW he has been developing microwave circuits with an emphasis on monolithic low noise HEMT amplifiers, low intermodulation distortion HBT amplifiers and MESFET/HEMT phase shifters. Currently he is developing phased array electronics at TRW.

Donald L. Tait (M'90) received the B.S. degree in geology from Michigan State University in 1981.

He was employed for a year as a Geophysicist for Geophysical Systems Inc. before falling victim to the oil glut. From 1983 to 1986 he was employed by J.E.F. Consultants developing microwave and millimeterwave antennas and their related components for automotive applications. He is currently employed as a Member of the Technical Staff by TRW Redondo Beach, CA, where his work has included low phase noise VCO's, HBT VCO's, HEMT amplifiers, high linearity HBT amplifiers and their applications.